Summary Phase III 2016

In the third phase of the project**: The efficiency control of the highorder harmonic generation and the optimal design of the deamdumps** we performed a theoretical analysis of the third order (THG) and fifth order (FHG) harmonic generation on CuI ablation plumes using high intensity laser pulses. The atoms (ions)-laser pulse field $E(t)=E_0(t)\sin(\omega_L t)$ interaction, ($E_0(t)$ being the on-off switching of the pulse profile at frequency ω_L) is described in the single active electron approximation with one electron constrained in its motion to the surface of a rigid sphere (with R radius) by solving the time-dependent Schrödinger equation: $i\hbar\frac{\partial|\psi(x,t)\rangle}{\partial t}=\hat{H}|\psi(x,t)\rangle$, where: $\hbar=h/2\pi=1{,}054\cdot10^{-34}$ J·s represents the reduced Planck's constant, $|\psi(x,t)\rangle$ is the full time-dependent wave function of the active electron acted upon by the laser field. In Eq. (1) the Hamiltonian is written in the form: $\hat{H}=\hat{H}_0+\hbar\cos\Omega_0(t)\sin(\omega_L t)$,where: $\hat{H}_0=(\hbar^2\hat{L}^2)/(2I)$ is the Hamiltonian of the atom (ion) in the absence of a laser field, $\hbar\Omega_0(t)=eRE_0(t)$, $I=m_eR^2$ is the moment of inertia of the electron, and $\hat{L}^2$ is the angular momentum operator squared, whose eigenstates are the usual spherical harmonics $Y_{l,m}(\theta,\phi)\rightarrow|l,m\rangle$, l being the orbital angular momentum, and m is the quantum number of the angular momentum projection.

Based on the theoretical model presented in literature it is convenient to write the full time-dependent wave function of the active electron at time t, as a linear combination of eigenstates of the laser-free Hamiltonian as: $|\psi(x,t)\rangle=\sum_{l'=0}^{\infty}\sum_{m'=-l}^{l}a_{l',m'}(t)|l',m'\rangle$, where $a_{l',m'}(t)$ are the expansion coefficients to be found by substitution into the time-dependent Schrödinger equation. Considering that $|\Lambda,m\rangle$ is the initial state for the highest-occupied atomic (ionic) orbital; according to the previous discussion, the laser field will couple only states with $m=m'$, finally one obtained the folowing equations:

$$i\dot{a}_{\Lambda,m}(t)=\omega_\Lambda a_{\Lambda,m}+\Omega_0(t)b_{\Lambda,m}\sin(\omega_L t)a_{\Lambda+1,m}$$

$$i\dot{a}_{l>\Lambda,m}(t)=\omega_l a_{l,m}+\Omega_0(t)\sin(\omega_L t)\left(b_{l-1,m}a_{l-1,m}+b_{l,m}a_{l+1,m}\right)$$

where: $b_{l,m}=\sqrt{\frac{(l+m+1)(l-m+1)}{(2l+1)(2l+2)}}$.

Since the energy gap increases with l, one can argue that the population of the upper levels becomes negligible; thus, the energy levels with quantum numbers $l>\Lambda+N'$ do not participate in the dynamics of the system. The set of differential equations (7), (8) shows a ladder-like structure, so that any energy level is coupled to the two adjacent levels. This system can be numerically solved by utilizing a Matlab numerical routine.

After the probability amplitudes $a_{k,m}$ are obtained one can calculate the matrix element of the electric dipole moment $er(t)$ induced by the laser field in the form:

$$r(t)=\langle\psi(t)|R\cos\theta|\psi(t)\rangle=R\sum_{s=0}^{\infty}b_{\Lambda+s,m}\left[a^*_{\Lambda+s,m}a_{\Lambda+s+1,m}+a_{\Lambda+s,m}a^*_{\Lambda+s+1,m}\right]$$

R being the atom radius.

We considered an electron constrained over a spherical surface (i. e.: CuI ([Ar] 3d(10) 4s(1)). For 5 mJ pump energy of a Nd:YAG laser (1064 nm wawelength) we obtained the maximum conversion efficiency for FHG: at 0.58 m and THG: at 0.64 m (Fig. 1), and in scale time for FHG: at 1.9 as and THG: at 2.8 ns (Fig. 2).

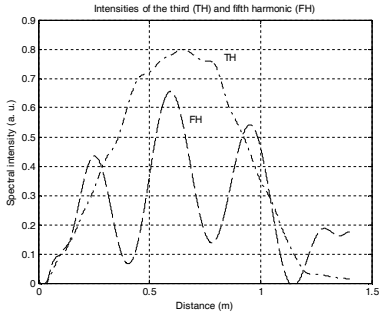

Fig. 1.

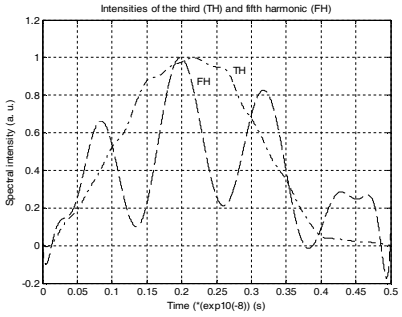

Fig. 2.

The optimum pressure within the laser focus (i.e. z=0) for phase matching between the fundamental radiation and *q*-th order harmonic is given by the relation: $p = p_0 \dfrac{\lambda_L^2}{2\pi^2 w_0^2 \left(n - n_q\right)\left(1 - \dfrac{\chi_e}{\chi_c}\right)}$. Here, $2w_o$ is the laser spot diameter in focus, χ_e denotes the ionization degree, χ_c is the critical ionization degree (i.e. the ionization degree at which the plasma dispersion due to the free electron exceeds the atomic dispersion) and p_o is the standard pressure. Figure 3(a) presents the calculated optimum pressure of N2 atmospheric gas at different χ_e/χ_c ratios for generating efficiently a low order harmonic (e.g. the third and fifth harmonics). The dispersion properties of nitrogen (N) for the very large spectral domain of interest here (i.e. from IR to VUV domain) are derived from several sources.

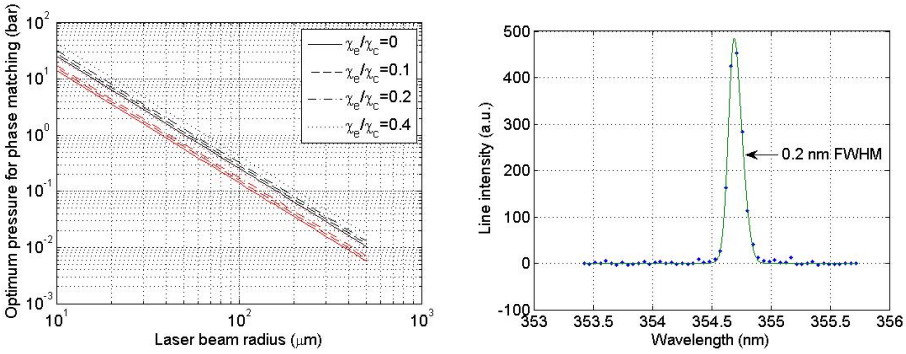

(a) (b)

Fig. 3 (a) Phase matching pressure versus beam radius for the harmonics H3 (black curves) and H5 (red curves) of the fundamental 1064 nm wavelength employing N as the generating medium at different ionization degrees**. (b)** Third harmonic obtained in air nitrogen by focusing 1064 nm, 5 ns laser pulses at peak intensity of 1TW/cm2

The net *q*-th harmonic photon yield is demonstrated to be directly related to square of pressure and medium length along the propagation direction of the radiation, according to the following relationship: $N_q \sim A\left(pL\right)^2$, where *A* is spot area of the pump beam at the interaction region. One can see that, in order to obtain high conversion efficiency for the q-th harmonic, we need to carefully control the following parameters: the irradiation geometry - a loose focusing conditions gives large laser spot area in focus and long focus *L* within the conversion medium which are effective conditions for the harmonic generation; the conversion pressures for the q-th harmonic - a high conversion pressure could be obtain by inducing ionization of the gas up to the critical level.

We further analysed experimentally the process of third harmonic generation in air nitrogen by using Nd-YAG laser pulses (1064 nm wavelength, 5 ns) focused in open air to a laser spot radius of 20 microns and a peak intensity of ~1TW/cm2. The frequency up-converted radiation was analysed in the axial direction (i.e. along the pumping fundamental beam) with an Ocean Optics HR2000+ spectrometer (0.1 nm FWHM resolution)- Fig. 3(b). The driving fundamental beam was reflected out of the radiation before reaching the spectrometer fiber tip by using a dichroic mirror. Since the collecting fiber tip was set ~40 cm away from the laser focus, we demonstrate the collimation property of the radiation at 354.7 nm wavelength (corresponding to the third harmonic of the fundamental pulses). The 3rd harmonic line has a Gaussian profile, the spectral width being ~0.2 nm FWHM.

In 2015 - 2016, the geometry of the most difficult experimental areas of the ELI-NP building was written according to the drawing files of the ELI-NP project (see figure 4, complete with designed beam dumps and local shielding). Initially it comprised the walls with penetrations (doors, laser transport beamlines, beamline at ERA, etc), and the interaction chambers. A shielding assessment of the individual experiments at E1/E6, E4, E5 of the HPLS and ERA of the GBS was conducted. We used updated source terms in order to compute ambient dose equivalent rates throughout the above mentioned experimental areas, we designed beamdumps for each of them and we checked the compliance of the simulation results with legal dose constraints. In figure 5 an example of is given for the worst electron source term - 38 GeV Gaussian gamma beam. Fluence rates of secondary photons, neutrons, protons, electrons and positrons, muons were scored in order to facilitate an optimum selection of the material and geometrical layout of the local shielding. An example can be seen in figure 6, for the intense electron beam at ERA. In each case a beamdump was proposed to stop the ionizing radiation with a minimum cost in activation. Several materials and geometrical displays were tried out in each case, before getting the final solution presented here. For those sources characterized by high current and high divergence, local shielding was added, in order to get the predicted equivalent dose rates below the admitted values.

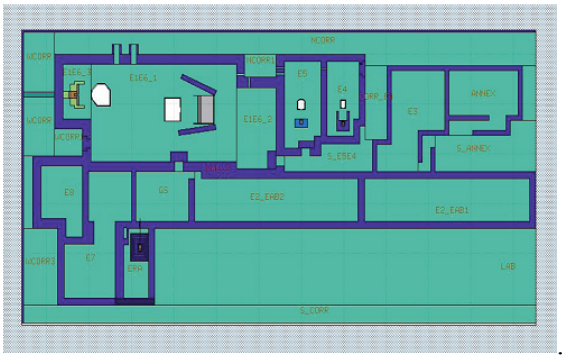

Fig. 4. Final FLUKA geometry of the experimental ELI-NP building complete with designed beamdumps and local shielding.

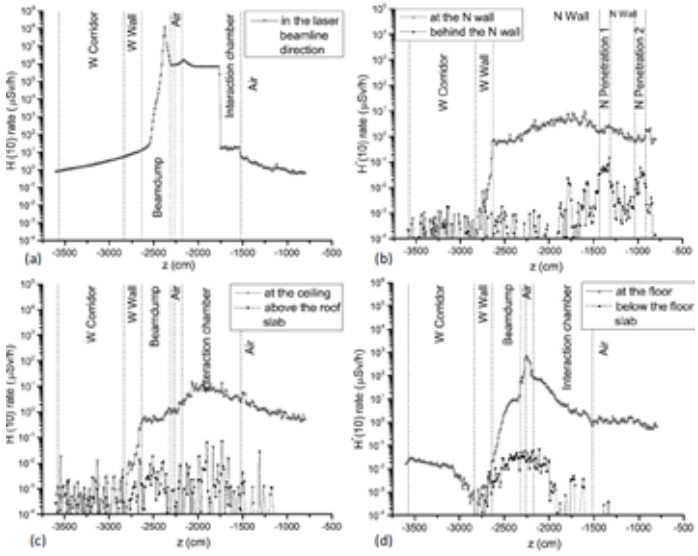

Total $H^*(10)$ rate (in μSv/h) generated by the 38 GeV electron beam (SE1) in the volume of a 20cm x 20 cm (xy section) column which spans the length of the geometry (z direction) and is located: (a) in the beamline direction, 150 cm above the floor; (b) at the same height, in front of and behind the north wall, where the main laser penetrations are lying; (c) above the beamline, at the ceiling level and above th roof slab, correspondingly; (d) below the beamline, at the floor level and below the floor slab (in the basement). For spatial orientation, the limits of the occupied areas were marked by vertical lines and regions were labeled.

Fig. 5.

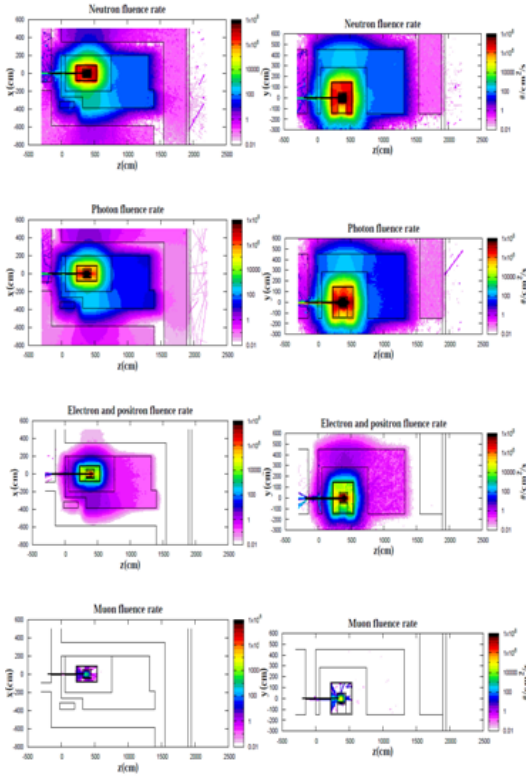

Particle fluence rate (#/cm^2/s) generated by the intense electron beam at ERA in a 20cm x 20cm cross section sampling volume centered on the beamline. A number of $1.\times10^{11}$ electrons/ pulse was considered at a pulse repetition rate of 100 Hz.

Fig. 6.

In this study typical source terms were used in the real geometry to assess existing bulk shielding and to propose beamdumps and local shielding of the experiments. The results can be used in the current design phase of the experiments. An analysis of activation at the most difficult, from a radioprotection point of view, experimental hall (E6) for beamdump components, walls, ambient air, interaction chamber and optical bench was conducted for planning intervention in the experimental area after ending an experiment.

References

1. *Radiation protection aspects at the electron recovery area of the ELI-NP Gamma Beam System*, M.A. Popovici, I.O. Mitu, Gh. Cata-Danil, accepted for publication in University "Politehnica" of Bucharest, Scientific Bulletin, Series A: Applied Mathematics and Physics
2. *Radiation Protection at ELI-NP*, I.O. Mitu, C. Ivan, F. Negoita, D. Aranghel, S. Bercea, E. Iliescu, C. Petcu, M. Gugiu, M.A. Popovici, C.A. Ur, S. Gales, N.V. Zamfir, Romanian Reports in Physics, Vol. 68, Supplement, P. S885–S945, 2016
3. *Shielding assessment of high field (QED) experiments at ELI-NP 10 PW laser system*, M. A. Popovici, I.O. Mitu, Gh. Cata-Danil, F. Negoita, C. Ivan, sent for publication to Journal of Radiological Protection
4. *Radiation protection evaluations for the ELI-NP facility with FLUKA Monte Carlo code*, M.A. Popovici, Gh. Cata-Danil, invited paper, accepted for the 3-rd International Conference on Computational and Experimental Science and Engineering (ICCESEN-2016), 19-24 Oct 2016, Antalya-Turkey